Journal of Non-Crystalline Solids 356 (2010) 777–781

Contents lists available at ScienceDirect

Journal of Non-Crystalline Solids

journal homepage: www.elsevier.com/locate/jnoncrysol

Relaxation and antiplasticization measurements in trehalose–glycerol mixtures – A model formulation for protein preservation

J. Obrzut [a,*], A. Anopchenko [a,1], J.F. Douglas [a], B.W. Rust [b]

[a] National Institute of Standards and Technology, Polymers Division, Gaithersburg, MD 20899, USA
[b] Mathematical and Computational Sciences Division, Gaithersburg, MD 20899, USA

ARTICLE INFO

Article history:
Available online 28 January 2010

Keywords:
Bioglass
Dielectric properties, relaxation, electric modulus

ABSTRACT

We utilize dielectric relaxation spectroscopy for the quantitative characterization of antiplasticization of glassy-trehalose by glycerol. The high frequency Johari–Goldstein relaxation time (τ) was obtained by analyzing the complex permittivity data in terms of the distribution function of relaxation times and a regularization technique. We analyzed the dielectric spectrum without prior assumptions about a spectral function and the number of the relaxation processes. The ratio of τ values for the mixture and pure trehalose, an antiplasticization factor (Θ), is found to provide a useful measure of the extent of antiplasticization. We observe that increasing the glycerol mass fraction (x_w) at fixed temperature increases τ, extending antiplasticization until a temperature dependent critical plasticization concentration is reached. At a fixed concentration, we find an antiplasticization temperature at which antiplasticization first occurs upon cooling. At a temperature of 293 K the antiplasticization factor peak value is about 1.6 when x_w of glycerol is about 0.24. At 323 K a mild antiplasticization maximum occurs when x_w decrease to about 0.05. Above 323 K, $\Theta < 1$, glycerol plasticizes trehalose, thus the antiplasticizing effect apparently no longer exists. The antiplasticization factor that we describe in terms of Arrhenius functions is a convenient predictive model to characterize antiplasticization in glassy sugar formulations and other glass-formers.

Published by Elsevier B.V.

1. Introduction

Sugar formulations are generally effective in preserving drugs and biological tissues [1,2]. Trehalose in particular has been widely used in preserving and maintaining the activity of diverse materials including proteins, viruses and antibodies [3]. A number of measurements and simulations have shown that the internal motions of proteins and other biological macromolecules tend to be strongly coupled to those of the glass solutions in which they are embedded [4,5]. The relatively high glass transition temperature of trehalose has been recognized as a factor enhancing the preservation time [6,7]. The amplitude of protein molecular motions can be further reduced by adding a small amount of glycerol to trehalose, improving the cryopreservation time [8,9]. This effect has been attributed to the antiplasticization of trehalose by glycerol, making the trehalose–glycerol mixture a stronger glass-former [10,11].

Antiplasticization in glassy polymers [12–14] is typically accompanied by reduction in glass transition, negative deviations from volume additivity upon mixing (i.e. the solutions densify upon mixing), an increase in elastic moduli [15,16], and suppression of the secondary relaxation. Antiplasticization has been observed in a number of polysaccharides mixtures [17–19] enriched by water and glycerol [20,21]. It was shown that glycerol slows down the secondary relaxation process of maltose up to concentrations of about 0.28 mass fractions. At higher concentrations of glycerol, the secondary relaxation process of maltose merges with the primary structural relaxation process of glycerol, and only plasticization is apparent [18]. Several studies have shown antiplasticization of trehalose by glycerol at various concentrations [22–24]. The antiplasticization effect was attributed to the formation of an extended network of hydrogen bonds with a longer lifetime at about 5% of glycerol [23]. It was also shown that at about 36% of glycerol, which corresponds to a stoichiometry of 2:1 glycerol to trehalose molecules, excess permittivity sharply increases indicating a change in dipole ordering from anti-parallel to parallel alignment [24]. However, to date there has been no strong evidence that glycerol increases the elastic moduli of glassy-trehalose that would be indicative of antiplasticization from the classical view point. In fact, molecular dynamics simulation showed that glycerol somewhat slows the mobility of hydrogen atoms on time scale of about 10^{-9} s, but the effect is small and does not influence the macroscopic elastic constants [25].

* Corresponding author.
E-mail address: jan.obrzut@nist.gov (J. Obrzut).
[1] Present address: Nanoscience Laboratory, University of Trento, via Sommarive 14, Povo, Trento 38100, Italy.

0022-3093/$ - see front matter Published by Elsevier B.V.
doi:10.1016/j.jnoncrysol.2009.07.045

In our previous work [24] we showed that antiplasticization in the trehalose–glycerol mixtures occurs only below a certain antiplasticization temperature (T_a), which corresponds to a compensation point between the enthalpic and entropic contributions to the free energy of activation. We characterized the extent of antiplasticization by using the relaxation time obtained from the Havriliak–Negami function under some arbitrary assumptions regarding the shape of the relaxation peak and the number of the relaxation processes. This typically leads to a conditioned solution, especially when the relaxation process results from mixing a secondary relaxation with an asymmetric primary relaxation, which is the case of glassy-trehalose and glycerol. In this work we employ a distribution function of relaxation times and a regularization technique to determine the relaxation time of the mix. This approach determines the relaxation time more accurately, without prior assumptions about a spectral function or about the number of the relaxation processes. We quantify the antiplasticization effect based on the measured relaxation time, and finally determine the temperature and concentration conditions using an Arrhenius function as a predictive model governing the antiplasticization.

2. Materials and measurements[2]

Anhydrous α, α′ trehalose and anhydrous glycerol were purchased from Sigma and Fluka, respectively, and used without further purification. The mixtures of trehalose and glycerol were prepared by dispersing glycerol in the trehalose powder followed by a homogenization at 350 K overnight. After mixing, the samples were melted at temperature of about 480 K and then cooled rapidly on a cold plate to obtain glassy transparent films. In order to avoid the caramelization of trehalose and the crystallization of the trehalose–di-hydrate, the samples were handled in an argon gas inert environment in the dry box.

We note that samples obtained by melting trehalose di-hydrate or subjected to freeze-drying, exhibit in their dielectric loss spectra an additional dielectric process in the intermediate frequency range between the β-relaxation and that characteristic of large scale structural α-relaxation. Though clearly absent in the glass mixtures obtained from amorphous trehalose prepared and handled in the moisture-free dry box [24], this feature appears on dielectric loss spectra with slowly growing intensity and drifting frequency over the time scale of several days when exposed to ambient humidity. We conclude that this additional relaxation originates from the residual crystalline trehalose–di-hydrate. Because the development of crystallinity has a clear signature in the NMR 25 MHz ^{13}C CPMAS spectrum [24], we use this technique as well to monitor the purity of our glassy materials.

2.1. Dielectric measurements

The dielectric permittivity data were obtained from the capacitance and loss tangent measurements in the frequency range of 100 Hz–100 MHz using an Agilent 4294A precision impedance analyzer. Solid film specimens, typically 200 μm thick were prepared in the dry box by melting samples between glass slides with evaporated aluminum electrodes, contacts, and spacers clamped together. After melting, the samples were cooled to obtain transparent glassy films. Liquid materials were injected to fill the gap between electrodes. The real part of the dielectric constant, ε' and the dielectric loss, ε'' were obtained from the measured complex capacitance and geometry of the test specimen. The relative standard uncertainty of the capacitance was assumed to be within the manufacturer's specification for the 4294A analyzer of 1%.

In the frequency range of 100 MHz–18 GHz, the dielectric permittivity was obtained from one-port reflection coefficient measurements, which were carried out with a HP 8720D vector network analyzer [26,27]. Dielectric measurements were carried in a nitrogen gas environment in the temperature range of 220–350 K. The specimen temperature was controlled to an uncertainty of ±0.5 K. The combined relative experimental uncertainty of the measured complex permittivity was within 8%, while the experimental resolution of the dielectric loss tangent measurements was about 0.005.

2.2. Calculations

The relaxation time was obtained by analyzing the complex permittivity data in terms of the distribution function of relaxation times and a regularization technique [28].

$$\frac{\varepsilon(\omega)-\varepsilon_\infty}{\Delta\varepsilon}=\int\frac{1}{1+i\omega\tau}G(\ln\tau)d(\ln\tau), \tag{1}$$

where $G(\ln\tau)$ is the logarithmic distribution function of relaxation times, $\varepsilon(\omega)$ is the complex permittivity, $\varepsilon=\varepsilon'-i\cdot\varepsilon''$, which depends on the angular frequency ω. $\Delta\varepsilon=\varepsilon_0-\varepsilon_\infty$ is the dielectric relaxation strength, ε_0 and ε_∞ are the relaxed and unrelaxed dielectric constant, respectively. Our data can be analyzed by a system of linear first kind integral Eq. (1) with additive random measuring errors. Here, we decompose the dielectric spectrum into several discrete processes with separated relaxation times without prior assumptions about a spectral function and the number of the relaxation processes. However, discretizing (1) leads to a regression problem in which the standard least squares estimate is unstable. In such cases, stable estimates are usually gotten by one of two general methods:

1. truncating a singular value decomposition (SVD) of the model matrix to remove components of the solution thought to be corrupted by measurement errors, or
2. appending additional linear equations to the model which describe *a priori* constraints, e.g., non-negativity that the unknown solution must satisfy.

The latter technique, which is usually called regularization, requires the user to choose a free parameter, which controls the relative weightings of the measurement equations and the additional constraint equations. In our calculations we have used a form of regularization where the regularization constraint was designed to smooth the estimate by making its second derivative vector close to the zero-vector [28,29]. The success of the regularization method depends crucially on the choice of the adjustable regularizing parameter. The criteria that we used to make this choice have been reviewed in Refs. [30,31]. The guiding principle is to seek estimates which produce residuals that are as much like the measurement errors as can be determined. For example, if the measurement errors are normally distributed, and the regression model is normalized to reduce the variance–covariance matrix to an identity matrix, then the residuals should be independently, identically distributed with a standard normal distribution, and the sum of squared residuals (SSR) should be a sample from a chi-square distribution with m degrees of freedom. The fact that the mean value of the above chi-square distribution is m suggests that one should seek an estimate which gives a SSR as close as possible to m. Other selection criteria that we used include generalized cross-validation, the L-curve method, and the length of the cumulative periodogram of the residuals [30,31]. The combined relative experimental uncertainty of the relaxation time was within 8%.

[2] Certain equipment, instruments or materials are identified in this paper in order to adequately specify the experimental details. Such identification does not imply recommendation by the National Institute of Standards and Technology nor does it imply the materials are necessarily the best available for the purpose.

3. Results and discussion

Fig. 1(a) illustrates the distribution function, $G(\ln\tau)$, for a series of trehalose–glycerol mixtures as well as for pure trehalose at 273 K. The peak of $\ln\tau$ at −13.5 in Fig. 1(a), plot (1) corresponds to a secondary relaxation in amorphous trehalose [24], where the relaxation time (τ) is about 1.5×10^{-6} s. We consider these relaxation time results more accurate than those previous reported from fitting to HN function, where the corresponding τ_{HN} was about 4.7×10^{-6} s.

To ensure that the obtained distribution functions are reliable (i.e. the spurious oscillations in the least squares estimate are damped out without biasing it too much toward the origin), we extracted the distribution of relaxation times for each mixture using three different numerical techniques. The results for trehalose are shown in Fig. 1(b) (the inset). Plot "s2d" shows the distribution function obtained by the regularization technique described in Section 2.2. Plot "tSVD" shows the result of the truncated singular component method [30,31] and the "Tikhonov" plot in Fig. 1(b) shows the results of a simple form of Tikhonov regularization, which is designed to make the least squares estimate close to the zero-vector. All three techniques result in the very similar distribution function, which supports the robustness of the regularization technique we use in this work.

The effect of 'antiplasticization' is seen in Fig. 1(a) as a shift of the relaxation peak towards longer relaxation time. At the temperature of 273 K, τ increases from 1.5×10^{-6} s to about 1.5×10^{-5} s when the mass fraction of glycerol is about 0.24. For higher glycerol concentration $x_w > 0.24$ the relaxation time starts to decrease (Fig. 1(a), plot (4), $\tau = 1.2 \times 10^{-5}$ s) the antiplasticization effect becomes weaker and eventually with the glycerol concentration increasing further, trehalose becomes plasticized by glycerol (Fig. 1a, plot (5)), $\tau = 2.3 \times 10^{-7}$ s). The antiplasticizing effect becomes more pronounced at low temperatures.

The temperature dependence of the relaxation time, τ, for pure trehalose and a series of trehalose–glycerol mixtures is shown in Fig. 2. The symbols correspond to τ data while the lines represent linear regression fit through the points. The relaxation time decreases with increasing temperature. For trehalose and mixtures with glycerol mass fraction (x_w) less than 0.5 the temperature dependence is well described by an Arrhenius function $\tau = \tau^{\#}\exp(E_A/RT)$, and is characteristic of a secondary β-relaxation process. The activation energy for the pure trehalose, $E_{A\text{-}trh}$, approximately equals 58 kJ/mol, which fits well with reports for other carbohydrates [20,21]. With increasing concentration of glycerol the activation energy of the mix, $E_{A\text{-}mix}$, increases, approaching the value of about 110 kJ/mol at the glycerol mass fraction of about $x_w \approx 0.5$. The concentration dependence of the activation energy and the corresponding relative pre-exponential factor ($\tau^{\#}_{mix}/\tau^{\#}_{trh}$) are plotted in the inset of Fig. 2. At higher glycerol concentrations, $x_w > 0.5$, the β-relaxation process becomes increasingly overlapped by the α-relaxation of glycerol and these plots show considerable curvature characteristic of the primary relaxation of the glycerol [24].

The extent of antiplasticization, i.e. an increase in the relaxation time upon mixing with glycerol, can be described quantitatively as a ratio of the relaxation time of the mix, τ_{mix}, to that of trehalose, τ_{trh}; $\Theta = \tau_{mix}/\tau_{trh}$. In Fig. 2, the points at which the relaxation time for the mixture τ_{mix} crosses the relaxation time for pure trehalose τ_{trh} represent conditions of $\Theta = 1$ at the characteristic antiplasticization temperature (T_a). Antiplasticization ($\Theta > 1$) occurs only at temperatures below T_a.

The physical interpretation of antiplasticization parameter Θ simplifies when the relaxation time is described by an Arrhenius temperature dependence, which is normally the case for β-relaxation processes. Since τ of trehalose and mixtures obeys the Arrhenius function (Fig. 2), we may express Θ as,

$$\ln(\Theta) = \ln\left(\frac{\tau^{\#}_{mix}}{\tau^{\#}_{trh}}\right) + \frac{(E_{A\text{-}mix} - E_{A\text{-}trh})}{R}\frac{1}{T}, \qquad (2)$$

where, $\ln(\Theta)$ is the natural logarithm of the antiplasticization factor introduced earlier, $\ln(\tau^{\#}_{mix}/\tau^{\#}_{trh})$ is a natural logarithm of the pre-exponential factors, R is the universal gas constant and T is the absolute temperature.

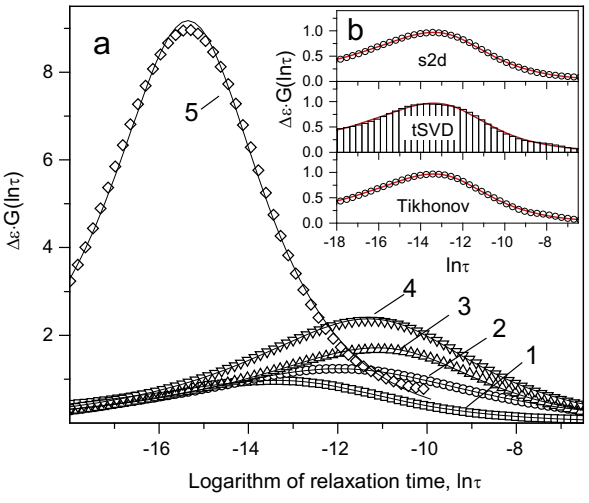

Fig. 1. (a) Relaxation spectra of the series of trehalose–glycerol mixtures, at 273 K; symbols – experimental data, lines – fits to the distribution function. (1) Trehalose; (2) $x_w = 0.15$; (3) $x_w = 0.24$; (4) $x_w = 0.36$, and (5) $x_w = 0.47$ mass fraction of glycerol. (b, inset) The distribution function of relaxation times for trehalose (Fig. 1a, plot (1)) obtained by three different numerical techniques: (s2d) a regularization technique to smooth the estimate by making its second derivative vector close to the zero-vector; (tSVD) truncated singular component method; (Tikhonov) a simple form of Tikhonov regularization to make the estimate close to the zero-vector.

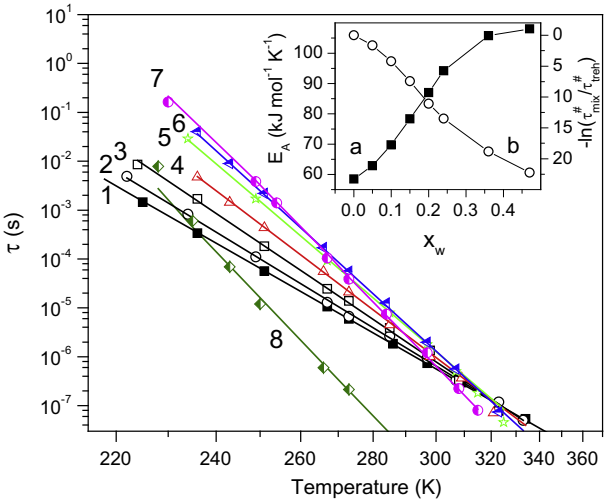

Fig. 2. Relaxation map for trehalose, plot (1), and for series of trehalose–glycerol mixtures at the following glycerol mass fraction: (2) $x_w = 0.05$, (3) $x_w = 0.10$, (4) $x_w = 0.15$, (5) $x_w = 0.20$, (6) $x_w = 0.24$, (7) $x_w = 0.36$, and (8) $x_w = 0.47$. The temperature axis is scaled as a reverse reciprocal ($1/T$). Inset shows activation energy (E_A), plot (a), and natural logarithm of the pre-exponential factors [$-\ln(\tau^{\#}_{mix}/\tau^{\#}_{trh})$], plot (b), as a function of the glycerol mass fraction.

Using Eq. (2) one can find the conditions for plasticization or antiplasticization. $\ln(\Theta) > 0$ corresponds to the antiplasticization conditions, which are most desirable from the bio-preservation point of view. In contrast, $\ln(\Theta) < 0$ corresponds to plasticization. The condition $\ln(\Theta) = 0$ at fixed concentration defines the antiplasticization temperature (T_a) while at fixed temperature it defines the plasticization concentration, x_{wp}. According to Fig. 2 (the inset), both the activation energy and the ratio of pre-exponential factors depend on glycerol concentration. The activation energy increases with the glycerol concentration, and thus the second term in Eq. (2), $(E_{A\text{-}mix} - E_{A\text{-}trh})/R$, is positive. On the other hand, $\ln(\tau^{\#}_{mix}/\tau^{\#}_{trh})$ decreases with x_w, and is always negative. Consequently, the *competition* between these two concentration trends in the activation energy and in the relaxation time pre-exponential factor leads to the peaking of antiplasticization as a function of x_w at a fixed temperature. Fig. 3 shows the solutions of Eq. (2) at several temperatures, illustrating the variation of $\ln(\Theta)$ as a function of x_w. For each temperature below 323 K (Fig. 3, plots (a–f)) there is well-defined concentration limit, x_{wp}, above which plasticization occurs ($\ln(\Theta) < 0$). Here, T_a defines a compensation temperature separating these two regimes. It is seen that above 323 K (Fig. 3, plots (g and h)) glycerol plasticizes trehalose. Thus for the trehalose–glycerol system the maximum antiplasticization temperature, $T_{a\text{-}max}$, is about 323 K. We see that at ambient temperature (293 K) the dielectric antiplasticization factor (Θ) approaches a maximum value of about 1.6 at x_w of 0.24 (Fig. 3, plot (d), $\ln(\Theta) \approx 0.5$) and it diminishes as the temperature increases and approaches $T_{a\text{-}max}$. The values of Θ in ambient conditions are rather small. Nevertheless, our measurement and analysis of the dielectric relaxation time indicate that glycerol suppress the local molecular motions in trehalose below $T_{a\text{-}max}$ and at $x_w < x_{wp}$. According to our earlier results [24], the NMR correlation time of about 2×10^{-6} s agrees well with the dielectric relaxation of pure trehalose, and thus, we concluded that the secondary relaxation in glassy-trehalose is governed by the small amplitude of delocalized motions involving the entire glucopyranose ring. On the other hand, the spectral density of molecular motions with correlation time where the dielectric measurements place the center of the β-relaxation, gives only a weak feature on the ^{13}C spectrum of glassy-trehalose. Similarly, molecular dynamics simulations showed that glycerol only slightly slows the mobility of hydrogen atoms on the time scale of about 1 ns [25]. Thus it seems that antiplasticization in sugars has its origin in subtle collective molecular motions [25,32], and it will therefore be interesting to consider the significance of Θ and T_a in relation to coupling between glass matrix and antiplasticizer in more detail.

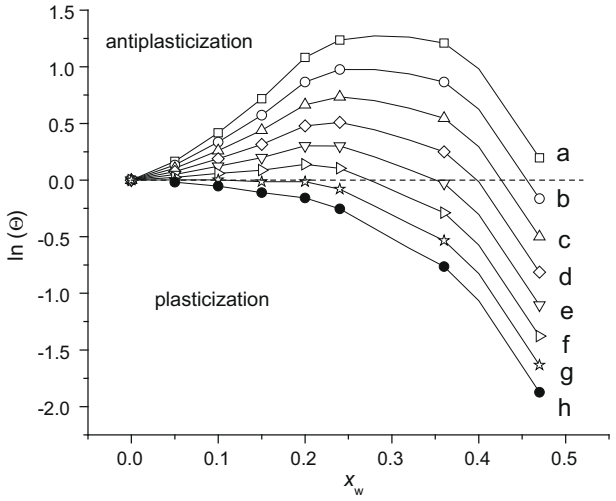

Fig. 3. Dielectric antiplasticization factor as a function of the glycerol mass fraction at the following temperatures: (a) 263 K, (b), 273 K, (c) 283 K, (d) 293 K, (e) 303 K, (f) 313 K, (g) 323 K and (h) 333 K. The horizontal line at $\ln(\Theta) = 0$ separates the antiplasticization and antiplasticization regimes.

The antiplasticization effect that we describe in our paper is certainly not restricted to applications relating to the preservation in sugar formulations. There is evidence for a plasticization-antiplasticization transition in the dynamics of synthetic polymer solutions where the addition of a polymer to a fragile polymer liquid, can either plasticize or antiplasticize the solvent to which they are added depending on concentration [33]. It is important to realize that this type of antiplasticization of glassy liquids only exists at low temperatures and that the same additive can plasticize rather than antiplasticize at higher temperatures above T_a. The temperature at which this change occurs evidently gives basic information for the effective preservation of biological materials as well as for the adjustment of the properties of synthetic glassy polymers.

4. Conclusion

We determined the relaxation time of trehalose–glycerol mixtures without ambiguity using the distribution function of relaxation times and regularization techniques. Glycerol suppresses the secondary relaxation and antiplasticizes trehalose. We quantify this antiplasticization effect by analyzing the secondary relaxation time of trehalose as function of temperature and glycerol concentration x_w. To measure the extent of antiplasticization, we introduced the dielectric antiplasticization factor (Θ) defined as the ratio of the relaxation times of the mixture to the relaxation time of pure glassy-trehalose, and employed the Arrhenius function as a predictive model of antiplasticization. The antiplasticization ($\Theta > 1$) occurs only below a certain antiplasticization temperature (T_a) and at glycerol concentration smaller than x_{wp}. Our findings indicate that glycerol is a weak antiplasticizer of trehalose in the temperature range where bio-preservation is most desirable.

References

[1] N. Guo, I. Puhlev, D.R. Brown, J. Mansbridge, F. Levine, Nat. Biotechnol. 18 (2000) 168.
[2] Y.C. Song, B.S. Khirabadi, F. Lightfoot, K.G.M. Brockbank, M.J. Taylor, Nat. Biotechnol. 18 (2000) 296.
[3] J.H. Crove et al., Stabilization of mammal cells in solution, in: J.M. Baust, J.G. Baust (Eds.), Advances in Biopreservation, Taylor and Francis, 2006 (Chapter 14).
[4] A. Ansari, C.M. Jones, E.R. Henry, J. Hofrichter, W.A. Eaton, Science 256 (1992) 1796.
[5] A.L. Tournier, J. Xu, J.C. Smith, Biophys. J. 85 (2003) 1871.
[6] M.T. Cicerone, J. Obrzut, A. Anopchenko, C.L. Soles, Bulletin of the American Physical Society, Annual APS March Meeting 2003, Austin, TX, March 3–7, 2003.
[7] K. Kawai, T. Hagiwara, R. Takai, T. Suzuki, Pharm. Res. 22 (2005) 490.
[8] G. Caliskan, A. Kisliuk, A.M. Tsai, C.L. Soles, A.P. Sokolov, J. Chem. Phys. 118 (2003) 4230.
[9] M.T. Cicerone, C.S. Soles, Biophys. J. 86 (2004) 3836.
[10] J. Dudowicz, K.F. Freed, J.F. Douglas, J. Chem. Phys. 123 (2005) 111102.
[11] R.A. Riggleman, J.F. Douglas, J.J. de Pablo, Phys. Rev. E 76 (2007) 011504.
[12] W.J. Jackson Jr., J.R. Caldwell, Adv. Chem. Series 48 (1965) 185. J. Appl. Polym. Sci. 11 (1967) 211.
[13] P. Bergquist, Y. Zhou, A.A. Jones, P.T. Inglefield, Macromolecules 32 (1999) 7925.
[14] K.L. Ngai, R.W. Rendell, A.F. Yee, D.J. Plazek, Macromolecules 24 (1991) 61.
[15] L.M. Robeson, Polym. Eng. Sci. 9 (1969) 277.
[16] Y. Maeda, D.R. Paul, J. Polym. Sci. B 25 (1987) 957. 25 (1987) 981; 25 (1987) 1005.
[17] D. Lourdin, S.G. Ring, P. Colonna, Carbohydr. Res. 306 (1998) 551.
[18] D. Lourdin, P. Colonna, S.G. Ring, Carbohydr. Res. 338 (2003) 2883.
[19] T.R. Noel, S.G. Ring, M.A. Whittam, J. Phys. Chem. 96 (1992) 5662.
[20] J. Einfeldt, D. Meißner, A. Kwasniewski, Prog. Polym. Sci. 26 (2001) 1419.
[21] J. Einfeldt, D. Meißner, A. Kwasniewski, L. Einfeldt, Polymer 42 (2001) 7049.
[22] J.E. Curtis, T.E. Dirama, G.A. Carri, D.J. Tobias, J. Phys. Chem. 110 (2006) 22953.
[23] T.E. Dirama, G.A. Carri, A.P. Skolov, J. Chem. Phys. 122 (2005) 114505.
[24] A. Anopchenko, T. Psurek, D. VanderHart, J.F. Douglas, J. Obrzut, Phys. Rev. E 74 (2006) 031501.

[25] R.A. Rigtleman, J.J. De Pablo, J. Chem. Phys. 128 (2008) 224504.
[26] J. Obrzut, A. Anopchenko, IEEE Trans. Instrum. Meas. 53 (2004) 1197.
[27] J. Obrzut, A. Anopchenko, R. Nozaki, in: Proceedings of the IEEE Conference on Instrumentation and Measurement, 16–19 May 2005, Ottawa, Canada, vol. 2, 2005, p. 1530.
[28] H. Schäfer, E. Sternin, R. Stannarius, M. Arndt, F. Kremer, Phys. Rev. Lett. 76 (1996) 2177.
[29] F. Alvarez, A. Alegría, J. Colmenero, J. Chem. Phys. 103 (1995) 798.
[30] B.W. Rust, Comput. Sci. Stat. 32 (2000) 333.
[31] B.W. Rust, D.P. O'Leary, Inverse Probl. 24 (2008) 034005.
[32] S. Shirke, P. Takhistov, R.D. Ludescher, J. Phys. Chem. B 109 (2005) 16119.
[33] S.L. Anderson, E.A. Grulke, P.T. DeLassus, P.B. Smith, C.W. Kocher, B.G. Landes, Marcromolecules 28 (1995) 2944.